

CEBAF Program Advisory Committee Seven Update Cover Sheet

This proposal update must be received by close of business on November 23, 1993 at:

CEBAF

User Liaison Office

FAX: (804) 249-5800

12000 Jefferson Avenue

Newport News, VA 23606

Present Conditionally Approved Proposal Title and Number

Measurement of Proton Polarization in the (p, p') Reaction

E 89-019

Contact Person

Name: Ron Gilman

Institution: Rutgers University

Address: P.O. Box 849, Dept Physics & Astronomy

Address: Piscataway, NJ 08855-0849

City, State ZIP/Country:

Phone: (908) 932-5489

FAX:

E-Mail → Internet: GILMAN@RUTHEP.Rutgers.edu

Experimental Hall: A

Total Days Requested for Approval: 28

Minimum and Maximum Beam Energies (GeV): 0.8-2.8

Minimum and Maximum Beam Currents (μ Amps): 10-30, 60

CEBAF Use Only

Receipt Date: 11/23/93

PR 93-101

By: _____

MEASUREMENT OF PROTON POLARIZATION
IN THE $d(\gamma, \bar{p})n$ REACTION

P. Bosted

AMERICAN UNIVERSITY

S. J. Freedman, D. F. Geesaman,

R. J. Holt (Spokesperson), H. E. Jackson,

C. E. Jones, D. Krakauer, D. Potterveld, B. Zeidman

ARGONNE NATIONAL LABORATORY

B. Filippone, R. D. McKeown

CALIFORNIA INSTITUTE OF TECHNOLOGY

J. Gomez, J. LeRose, R. Michaels, S. Nanda, A. Saha

CONTINUOUS ELECTRON BEAM ACCELERATOR FACILITY

E. Kinney

UNIVERSITY OF COLORADO

P. Rutt

UNIVERSITY OF GEORGIA AND RUTGERS UNIVERSITY

G. G. Petratos

KENT STATE UNIVERSITY

E. Beise

UNIVERSITY OF MARYLAND

R. Milner

MASSACHUSETTS INSTITUTE OF TECHNOLOGY

K. P. Coulter

UNIVERSITY OF MICHIGAN

R. E. Segel

NORTHWESTERN UNIVERSITY

L. Bimbot

IPN ORSAY AND RUTGERS UNIVERSITY

J. Napolitano

RENSSELAER POLYTECHNIC INSTITUTE

D. Beatty, E. Brash, R. Gilman (Spokesperson), C. Glashauser

G. Kumbartzki, R. Ransome

RUTGERS UNIVERSITY

L. Auerbach, J. Martoff, Z.-E. Meziani (Spokesperson)

TEMPLE UNIVERSITY

D. Beck

UNIVERSITY OF ILLINOIS

120-80 84

I. ABSTRACT

We propose to measure proton polarizations in the reaction $d(\gamma, \vec{p})n$ for photon energies from 0.8 to 2.8 GeV and a range of angles. Existing cross section data exhibit an energy dependence near 90°_{cm} consistent with that expected for asymptotic scaling, for photon energies above about 1.3 GeV. The energy dependence is not reproduced over the range of the data by conventional nuclear calculations. The proton polarization should be a sensitive test of the reaction mechanism, since scaling requires zero polarization, whereas rescattering in the nuclear models generally implies nonzero polarizations.

II. QUARK SUBSTRUCTURE MOTIVATION

II.a The $d(\gamma, p)n$ Reaction

The $d(\gamma, p)n$ reaction is the simplest test case for nuclear-physics theory. The deuteron is the simplest nucleus, and allows the best separation of nuclear-structure ambiguities from reaction-mechanism ambiguities. As the incident γ energy is raised, new degrees of freedom become important, perhaps even dominant. In the intermediate-energy regime, it is important to consider Born terms, final-state NN interactions (FSI), isobar configurations, and meson-exchange currents. As energy and momentum transfer increase, this physical picture may break down, and it may be both necessary and more efficient to describe reactions in terms of quarks and gluons, the substructure of the nucleons.

Evidence for this subnucleonic picture may already exist in cross section measurements[1] of deuteron photodisintegration up to 1.8 GeV photon energy. More recent measurements[2] have extended the range of the data to 2.8 GeV at 90°_{cm} . These measurements (see Figure 1) are in agreement with the simple counting behavior of $d\sigma/dt \approx 1/s^{n-2}$, where n is the number of fundamental constituents (quarks, photons, leptons...) in the initial and final states. The measurement of polarization observables will provide a more sensitive test, since helicity conservation requires[3] that nucleon polarizations be zero in $d(\gamma, \vec{p})n$.

In general, it is expected that the onset of scaling requires large values for all the Mandelstam variables, s , t , and u . [4] Thus, for fixed incident energy, the physical picture may change from scaling behavior near 90°_{cm} to nonscaling behavior at the forward and backward angles. Indeed, this appears to be the case for $d(\gamma, p)n$ - see Figure 2. If we estimate simply that scaling starts at $t = u = 1.0 (\text{GeV}/c)^2$ per quark, or $3 (\text{GeV}/c)^2$ for the nucleon, at 90°_{cm} , then we require $s \approx 11 \text{ GeV}^2$, and $E_\gamma \approx 2.1 \text{ GeV}$. This is considerably higher than the suggested onset of scaling for $d(\gamma, p)n$. At $E_\gamma \approx 1.3 \text{ GeV}$ and 90°_{cm} , $t = u = 0.5 (\text{GeV}/c)^2$ per quark and $s \approx 8 \text{ GeV}^2$. However, the onset of scaling is controversial and the

limit suggested above is not universally accepted. The current experiment will measure polarizations at 90°_{cm} , for $-t$ from 0.6 to 4.3 (GeV/c)².

II.b pp Elastic Scattering

It is known[5] that pp elastic cross sections fall as $d\sigma/dt \approx s^{-10}$ at constant center of mass angle for $s > 15 \text{ GeV}^2$, equivalent to an incident kinetic energy of about 6 GeV, and $-t > 2.5 \text{ GeV}^2$, equivalent to a scattering angle of almost 60°_{cm} at the limiting value of s . This is generally accepted as evidence for scaling, since scaling predicts the exponent should be -10. We now turn to polarization measurements for s and t larger than the limits suggested by the cross section scaling.

The best evidence against scaling is the analyzing power measurements[6] at 24 and 28 GeV/c incident proton momentum, corresponding to $s = 46.8$ and 54.4 GeV^2 . These data show that for p_\perp^2 from about 3 to 7 (GeV/c)², corresponding to $-t$ ranging from 3 to 9 (GeV/c)², the analyzing power increases approximately linearly with p_\perp^2 from about 0.0 to 0.2, with uncertainties as small as 0.05. The scaling prediction is an analyzing power of zero. Although we would naively expect it to hold for these kinematics, the disagreement is evident.

Other data in the scaling regime are either consistent with scaling, or exhibit disagreement that is statistically marginally significant. For example, Fidencaro *et al.*[7] show data for $-t$ between 2 and 4 (GeV/c)². The polarization is consistent with zero, with an average of about 0.05 for a typical uncertainty of about 0.10. Crosbie *et al.*[8] show several high t data points at 90°_{cm} , for which the analyzing power must be zero due to symmetry. They also show one data point at 11.75 GeV/c incident momentum and 70°_{cm} ($s = 23.9 \text{ (GeV)}^2$, $t = -6.7 \text{ (GeV/c)}^2$, $u = -13.7 \text{ (GeV/c)}^2$), for which the analyzing power is $4 \pm 2\%$. Most of the data from Khiari *et al.*[9] are outside the expected scaling regime, or concerns double polarization parameters, for which the predictions are less clear. (A detailed discussion of this is presented in reference 8.) The analyzing power at incident momentum of 18.5 GeV/c and $-t = 5.6 \text{ (GeV/c)}^2$ is 0, as required in the scaling regime. An angular distribution for incident momentum of 11.75 GeV/c ($s = 23.9 \text{ GeV}^2$) has data for $-t$ between 3 and 10 (GeV/c)², equivalent to p_\perp^2 between 2.5 and 5.0 (GeV/c)². The upper limit corresponds to 90°_{cm} . All data are consistent with an analyzing power of about 2%, with similar sized uncertainties.

However, it turns out that pp elastic scattering is probably not a good case for exploration of the onset of scaling. The independent quark scattering Landshoff amplitude[10] – see Figure 3 – is expected to fall off with energy at about the same rate as the short-range hard scattering asymptotic amplitude. Since the Landshoff amplitude can induce polarizations at high momentum transfer, pp elastic scattering can generally be expected to show some polarization ef-

fects. While the relative contributions of Landshoff and asymptotic amplitudes are difficult to evaluate from theory, fits to pp scattering data seem to indicate the Landshoff amplitude can dominate over the asymptotic amplitude in some exclusive channels.

II.c Quark Substructure Conclusion

In the above sections, we have shown that cross sections for $d(\gamma, p)n$ are indicative of scaling. We have also examined pp elastic scattering, which has been suggested as evidence of scaling behavior on the basis of the energy dependence of the cross sections. We have concluded that polarization data contradict the simplest interpretation of scaling, and that the Landshoff amplitude in pp scattering may be large and explain the polarization effects.

Although we have not examined other cases at all, we note that a number of other reactions and the nucleon electromagnetic form factors have also been proposed as evidence of scaling. In all these cases, the behavior of the data at large momentum transfer is consistent with scaling predictions. However, theoretical interpretations of these data are not simple, and there are strong theoretical arguments against the scaling interpretation. An excellent summary of much of the data and theoretical arguments can be found in Isgur and Llewellyn Smith[11].

We conclude that the onset of scaling in these phenomena remains an interesting, and open question. In the case of deuteron photodisintegration, there is no Landshoff amplitude which can induce polarization. Thus, the proton polarization that we propose to measure will be a definitive test. Scaling requires a polarization of zero, and the measurements will be in the kinematics for which the cross sections indicate scaling behavior.

III. NUCLEAR PHYSICS MOTIVATION

In the previous section, we have described why the $d(\gamma, \vec{p})n$ reaction is interesting to measure, from the consideration that the relevant degrees of freedom may be those of quarks and gluons, and that the onset of scaling behavior is interesting to either confirm or repudiate. In this section, we give a qualitative description of the reaction from a nuclear physics perspective, make a simple prediction for the proton polarization, and indicate some of the sensitivities of the data to the reaction mechanism.

For lower energies, the relevant degrees of freedom for the $d(\gamma, p)n$ reaction are those of nucleons, baryon resonances, and mesons. A simple picture of the reaction mechanism involves two steps. First, there is resonant and nonresonant absorption of the incoming photon on one of the nucleons in the deuteron. Second, rescattering of the two nucleons results in a sharing of the photon's energy,

as well as deexcitation of any excited resonance. Clearly, there are a number of diagrams that must be included in a realistic theory. Important elements in nuclear calculations of the process include the various meson-baryon couplings, $n\gamma$ couplings to various resonances, the deuteron wave function (in particular at short distances), and the nn rescattering.

The issues mentioned briefly in the above paragraph have been discussed at length elsewhere[1,2,12], focussing particularly on the cross section predictions. For brevity, we will omit these discussions and concentrate on polarization predictions. The existing data for polarization measurements at four angles have been compiled and displayed in Figure 4. Sensitivity of the polarization to the nuclear wave function is shown at 90°_{cm} for the calculations of Laget.

In the simple mechanism described above, proton polarization may result from two sources. First, interferences between the various resonant and non-resonant amplitudes result in polarizations. This is responsible for the large polarizations seen in the data for photon energies in the range of several hundred MeV. Second, polarization may be induced in the np rescattering that shares energy between the two nucleons.

An important simplification in the nuclear picture may be that the resonance excitations in effect average out to have no effect on the predictions for cross sections for photon energies much greater than 1 GeV. This can be seen by looking at γp and γd total cross sections (see Figure 5), which vary smoothly with energy, showing no resonances that are strongly coupled to the incident γd state. Coupling to resonances in this region might still lead to large polarizations, however – it is difficult to assess this precisely since the couplings are not well known.

In the following paragraphs, we will neglect the contribution of resonance couplings to the polarization. The polarization will result only from the FSI. It is important to emphasize that in the nucleon / meson picture of the reaction, independent of the particular diagrams drawn, we know that the final-state np system requires an interaction between the two nucleons. In this picture, the nucleons must interact, and there must be a polarization. (Note the arguments from the discussion of pp scattering above. In general, polarization effects are expected from the Landshoff process up to very high energies / momentum transfers.) With the exception of 0 and 180° , for which there exist symmetry arguments requiring zero polarization, the polarization for $d(\gamma, p)n$ may be zero at a particular choice of kinematics, but must be generally nonzero. Observation of generally zero polarization is inconsistent with a nucleon / meson picture of the reaction.

These observations may be used to make an approximate prediction of the

polarization expected in $d(\gamma, \vec{p})n$. Figure 6 shows proton polarizations from Corcoran *et al.*[13]. In the kinematics of this experiment, the photon energy varies from 0.8 to 2.8 GeV, giving a variation in s from 6.5 to 14.0 GeV². Examining Figure 6, we see that for smaller values of $-t$, the polarization decreases by about a factor of two over this range of s , whereas the decrease is less for larger values of $-t$. Although polarization in $d(\gamma, \vec{p})n$ is induced by pn rather than pp scattering, we make a similar estimate that over the range of energies of this experiment (see Figure 4) polarization from FSI will decrease by about 50%. (In fact, polarizations calculated with phase shifts from Arndt for pn scattering corresponding to our lowest energy point are of magnitude 0.2 or greater across almost the entire angular range, peaking at about -0.6 near 110°.) If the meson / nucleon picture remained valid, only at $E_\gamma \approx 15$ GeV, corresponding to $s = 60$ GeV², would the FSI induced polarization would go to zero.

IV. PROPOSED MEASUREMENTS

We propose to measure $d(\gamma, \vec{p})n$ for a range of angles and photon energies from 0.8 to 2.8 GeV, in steps of 0.4 GeV. The proposed kinematics are shown in Table 1. We will use the focal plane polarimeter in the HRS spectrometer in Hall A to perform this measurement.

We have chosen to make the measurements at angles in the center of mass of 37°, 53°, 90°, and 114°. At the forward two angles, we will measure up to 2.4 GeV, the highest energy in which a precise polarization measurement may be made in a relatively short time. At 90°, we will measure up to 2.4 GeV, with good precision, and a point at 2.8 GeV with reduced precision, since this is the highest energy at this angle for the NE17 data, and about the highest feasible energy for the polarization measurement. At 114°, we will measure up to only 1.6 GeV, the highest energy for which data were taken in NE8 – this angle was not measured in NE17 and is not planned for CEBAF experiment 89-12.

The choice of angles has been made for maximum overlap with the existing data of SLAC experiments NE8[1] and NE17[2], and the proposed data for the Hall C experiment 89-12, by R. Holt and collaborators. We have also decided to avoid measurements at large angles, due to the low figures of merit that result from spin precession in the spectrometer. (Depending on the results of these experiments, we may in the future request time to continue these measurements at the larger angles. In this case, we expect to propose to equip the SOS spectrometer with a polarimeter, to make use of an improved figure of merit to reduce beam time needed.)

The energies chosen are compatible with the NE17 data, but not with the proposed energies for CEBAF experiment 89-12 (1.5 to 4.0 GeV in 0.5 GeV

steps). The basic motivation was to maximize time at energies compatible with operation of the CEBAF accelerator and Halls B and C at 4 GeV, with Hall A receiving a lower energy – either 0.8, 1.6, or 2.4 GeV. Intermediate energies were chosen to avoid too large energy steps, and 2.8 GeV was chosen as the maximum feasible energy. The 0.8 GeV energy provides overlap with existing polarization data.

V. EXPERIMENTAL TECHNIQUE

The basic experimental technique is as follows. The electron beam strikes a radiator, producing a 0° bremsstrahlung photon beam with maximum energy essentially equal to the electron kinetic energy. The target, located downstream of the radiator, is irradiated by both the photons and residual electrons. Outgoing protons from the photodisintegration, as well as background particles, are detected in the Hall A HRS spectrometer.

The only nonstandard piece of equipment is the radiator used to generate the bremsstrahlung beam. Note that, since the $d(\gamma, p)n$ reaction has only two bodies in either the initial or final state, the angle and energy measurement of the outgoing proton completely determines the energy and momentum vector of the neutron, as well as the incident photon energy. This kinematic fact, coupled to our measuring only protons from near the endpoint of the bremsstrahlung spectrum, allows the experiment to be run with the large nonmonochromatic bremsstrahlung photon flux.

The radiator will be a 6% of a radiation length Cu radiator, approximately 1 mm thick. The Cu will be placed in the scattering chamber at least 10 cm upstream of the cryotarget, so that the spectrometer does not view it directly at our most forward angles. Energy loss in the Cu is about 90 watts. While we do require a remote radiator changing mechanism, the device is fairly simple to build, and should not be a problem. Note that since our primary goal is the measurement of proton polarization, rather than a cross section, we are insensitive to the usual difficulty that Bremsstrahlung experiments have in knowing the photon flux precisely, so that a cross section may be derived.

The radiator does contribute to background in the Hall both through increased production of low energy neutrons and increased production of high energy pions, that can penetrate thick shielding. Based on estimates[14] of backgrounds at 4 GeV from these processes, the radiator will contribute perhaps a few kHz of singles rate to each scintillator in the detector stack, leading to almost no triggers.

Another consideration is the total amount of energy deposited in the Hall, which is limited by regulation. Since we plan to run a total target thickness (in-

cluding the 1.4% deuterium target) of about 7.4% at highest energy and current of 2.8 GeV and 60 μA , we are below the Hall A design limits of 3.0% target at 4.0 GeV and 200 μA . A better estimate[15] shows that our peak intensity is below the average allowed for the Hall. Since the experimental time is determined by luminosity limits rather than count rate limits, we would choose to run all but the lowest energy kinematics at a higher luminosity at the time of the experiment if that were to prove feasible.

The Hall A cryotarget is designed for heat loads up to 1 kW, much greater than the 200 W load for this experiment. While the cryotarget is currently de-scoped, a large fraction of the difficult aspects of the project have been completed by the California State University Los Angeles group. The cryotarget is also required by almost all approved Hall A experiments, and should be available for this one. At this heat load, the average temperature change of the target liquid should be much less than 1 K, so density fluctuations should be negligible. Too, density fluctuations do not affect the polarization measurement.

The proton spectrometer will be used in its standard configuration. The experiment as proposed is very clean of background, largely due to the kinematics chosen. Background particles from the deuterium target, including both πs and $d\text{s}$ from photon and electron induced reactions, have momentum much lower than the proton momentum in our proposed kinematics. These particles are not in fact transported through the magnet into the detectors because of their low momentum. The highest momentum protons from deuteron electrodisintegration will have the same momentum as the highest momentum protons from deuteron photodisintegration. These will have to be subtracted out by radiator in / radiator out comparisons. (In the conditions of NE8[1], photodisintegration yields were typically two to three times the electrodisintegration yields. We will conservatively assume a one to one ratio in making estimates for statistics.) When the disintegration is accompanied by π^0 production, the corresponding protons are lower in momentum by over 2% in our worst kinematics, compared to the protons of interest. Cuts on the proton momentum should be easy as long as the spectrometer works at the 10^{-3} level, an order of magnitude worse than the design goals. Thus, aside from the required radiator in / radiator out subtractions, background from the deuterium target is negligible.

Background particles may also come from the Al endcaps of the target. These should not be a problem, as the spectrometer design indicates 1 mm resolution in transverse position at the target. At our most forward angles, the apparent target width is about 3.5 cm, and 3 sigma cuts should remove essentially all the Al background rate while reducing the data rate less than 20 %. This problem will be less severe at larger angles. Nonetheless, we plan to measure some empty target

backgrounds if this information is not available from spectrometer development data.

An additional background known for long cryogenic targets used at SLAC is a two step background, involving interactions with two separate nuclei. From models of these processes, plus the experimental data of NE8 and NE17, we know that this background will not be seen in this experiment. The background increases at larger angles and higher energies, but it was not seen at 2.8 GeV and 90°_{cm} in NE17.

Except for the addition of a focal plane polarimeter (FPP), the experimental technique and energy range are similar to that of Experiments NE8 and NE17 at SLAC as well as the Hall C proposal 89-12. (There is also a large overlap between the current collaboration and those experiments.) The data from the SLAC experiments give confidence that the experimental technique, other than the use of the polarimeter, should be straightforward for the setup that we have proposed.

The FPP planned for Hall A is currently under construction by Rutgers University and the College of William & Mary. There is extensive experience measuring proton polarization with carbon FPPs, as is planned for Hall A, up to $T_p = 800$ MeV at Los Alamos and the other meson factories. There is excellent overlap (about 2 - 3% variations) between the calibrations of the various FPPs, leading to confidence that there should be no difficulty in operations at CEBAF up to 800 MeV kinetic energy. This range includes all of our data at 114° , points up to 1.6 GeV photon energy at 90° , and points at 0.8 and 1.2 GeV at 37° and 53° .

Various of the Hall A polarimetry experiments require measurements of the polarization for kinetic energies above 2 GeV. For these experiments, we plan to calibrate the FPP by measuring the $p(\vec{e}, e'\vec{p})$ reaction. The knowledge of magnetic and electric form factors of the proton up to $Q^2 = 4$ (GeV/c)², beam polarization, and spin transport, will allow the FPP to be calibrated for proton energies up to 2.1 GeV with good precision. This calibration should in principle agree with that of the the POMME polarimeter[16] at SACLAY. POMME has now been calibrated to kinetic energies greater than 2.0 GeV.

With the exception of one data point at 2 GeV, our highest energy points are at about 1.6 GeV. Given our precision requirements, it should be possible to simply import the POMME calibration for the current experiment. Note that even if there are large (5%) systematic problems in the calibration, the resulting proton polarization will be changed from, e.g., 0.20 to 0.19 or 0.21. Thus, this systematic uncertainty should not be important for this experiment.

Commissioning the polarimeter also involves a set of calibration runs to examine the detector alignment and response. False asymmetries from the device can be checked with unpolarized e^-p elastic scattering, which should yield zero polarization. Our design goal is to keep false asymmetries below the level of 0.005. With an analyzing power of about 0.2, this corresponds to a false polarization of 0.025.

In the discussion above, we have ignored the issue of spin transport. For $d(\gamma, p)n$ the proton polarization will be normal to the reaction plane. The longitudinal and sideways components, p_l and p_s , are zero. As the proton is transported through the spectrometer, the spin will precess about the magnetic field into the longitudinal direction, with the net precession resulting mostly from the dipole magnets. The precession angle is given by $\Xi = 1.79\omega\gamma$, where 1.79 is the numerical value of $g_p/2 - 1$, ω is the bend angle of the spectrometer, and $\gamma = E/m$ is the Lorentz factor. The precession angle is shown in Figure 7. For much of the kinematic range of the experiment, in particular for the higher energy points at 90°_{cm} , spin precession changes the direction of the protons polarization by almost 180° , so that the magnitude of the polarization is essentially as large at the focal plane as at the target.

Thus, the proton polarization in the detector stack will have both normal and small longitudinal components. Only the transverse polarization components are measured in the FPP, through the spin-orbit contribution to proton scattering from carbon. With $p_s = 0$, the proton scatters in the carbon block of the FPP with an angular distribution shape $I_o(\Theta)[1 + p_n A_c(\Theta)\cos(\phi)]$, where $I_o(\Theta)$ is the unpolarized angular distribution, A_c is the analyzing power of carbon, and ϕ is the azimuthal angle. The useful range in scattering angle Θ is typically 5° to 20° , for which $A_c \approx 0.2$ near 1 GeV kinetic energy, and falls slowly with energy.

From consideration of the points discussed above, we believe this experiment is appropriate for early running at CEBAF. Technical demands from the experiment are slight. Only the Hall A hadron spectrometer is required. Particle identification, energy resolution, and angular precision requirements are all modest, well below the design requirements of the equipment. The only exception is the transverse position resolution at the target, which we use to reduce the running time by removing the need for empty target subtractions. Power load on the cryotarget is modest. With respect to the polarimeter, we believe the precision of the calibration required is such that we could run the experiment before the FPP is calibrated onsite by the $p(\vec{e}, e'\vec{p})$ reaction. The major time dependence in FPP calibrations results from relative motions of the detectors, which can be moved. The analyzing power of the carbon does not change, and if needed, corrections from a subsequent calibration could be applied to the data.

VI. TIME ESTIMATES

Count rates have been calculated under the following assumptions. The cross sections for the $d(\gamma, p)n$ reaction are either known, or can be extrapolated from the scaling laws, for the kinematics proposed. We use a 10 cm (1.7 g/cm^2) liquid deuterium target. The beam current is $60 \mu\text{A}$ at all energies except 0.8 GeV, for which we use $10 - 30 \mu\text{A}$, depending on angle, to reduce the count rate. (Each of these points will require about one hour of beam time.) The photon flux is calculated for a 6% radiator. The HRS spectrometer has a solid angle of 7.0 msr, and is assumed to be 80% efficient at detecting particles. Polarimeter efficiency and analyzing power has been taken from the POMME data.

Statistical uncertainties have been determined from the following considerations. Systematic uncertainties on the polarization are about 0.025 from false asymmetries, 0.01 from the analyzing power calibration, and 0.01 from spin transport through the spectrometer, leading to a total systematic uncertainty of 0.03. Since the spin transport causes the polarization at the target and in the focal plane to be about equal in magnitude for much of our kinematics, these uncertainties also apply to the polarization at the target. We generally aim for a statistical uncertainty of about 0.05, larger but close to the systematic uncertainty. This number includes a contribution from subtraction of the electrodisintegration background, under the worst case assumption that the background rates equal the photodisintegration rates. Thus, the final uncertainties will generally be 0.05 statistical + 0.03 systematic.

We have decided to reduce running time and statistical precision on two points, essentially because these points have increased systematic uncertainties. For the point at 2.4 GeV and 37° , spin precession reduces the polarization by a factor of 4. This will lead to a systematic uncertainty after spin transport back to the target of about 0.10. Thus we reduce the statistical uncertainty also to 0.10. Similarly, the spin is reduced by about a factor of two for the highest energy point at 53° , and we decrease the statistics for this data point by a factor of two, increasing the uncertainty to about 0.07.

The resulting time estimates are shown in Table 1. The total time request, including time for electrodisintegration measurements, is 625 hours, equivalent to 26 days. We also request two additional days to make empty target background measurements for some of our data points, and to repeat some of the points with a thinner 3% radiator, so that subtractions may be checked. These measurements will be done during the data taking at the lower beam energies so as to minimize time required.

VII. COLLABORATION BACKGROUND AND RESPONSIBILITIES

Many members of the current collaboration were involved in the photodisintegration experiments NE8 and NE17 at SLAC. A significant fraction of the collaboration is also involved in the Hall C experiment, 89-12, to measure cross sections up to 4 GeV photon energy. The experiment has also been accepted into the Hall A collaboration, and includes individuals within Hall A responsible for developing the focal plane polarimeter (Rutgers, Georgia). All major components of the equipment are part of the standard package of equipment in Hall A.

VIII. REFERENCES

- [1] J. Napolitano *et al.*, Phys. Rev. Lett. **61**, 2530 (1988); S. J. Freedman *et al.*, Phys. Rev. **C48**, 1864 (1993); T. Y. Tung, Ph.D. dissertation, Northwestern University (1992).
- [2] R. Holt, NE17 Collaboration, private communication. See also *Two Body Deuteron Photodisintegration Up to 4 GeV*, Dave Potterveld, CEBAF 1992 Summer Workshop, in AIP Conference Proceedings No. 269, pg 291, 1993.
- [3] J. Ralston, private communication. D. Sivers, private communication. The general case for exclusive reactions has been proven by Carl E. Carlson and M. Chachkhunashvili, unpublished. The specific case for deuteron photodisintegration can also be easily seen by keeping only helicity-conserving amplitudes, as presented in, e.g., V. P. Barannik *et al.*, Nucl. Phys. **A451**, 751 (1986).
- [4] Discussions of scaling may be found in, e.g., S. J. Brodsky and G. R. Farrar, Phys. Rev. Lett. **31**, 1153 (1973); V. A. Mateev *et al.*, Lett. Nuovo Cimento **7**, 719 (1973); S. J. Brodsky and G. R. Farrar, Phys. Rev. D **11**, 1309 (1975). The physics has also been extended for the deuteron photodisintegration case with the reduced nuclear amplitudes model in S. J. Brodsky and J. R. Hiller, Phys. Rev. C **28**, 475 (1983).
- [5] P. V. Landshoff and J. C. Polkinghorne, Phys. Lett. **44B**, 293 (1973).
- [6] see D. G. Crabb *et al.*, Phys. Rev. Lett. **65**, 3241 (1990), and references therein.
- [7] G. Fidecaro *et al.* Phys. Lett. **105B**, 309 (1981);
- [8] E. A. Crosbie *et al.* Phys. Rev. D **23**, 600 (1981).
- [9] F. Z. Khiari *et al.* Phys. Rev. D **39**, 45 (1989).
- [10] see C. E. Carlson, M. Chachkhunashvili, and F. Myhrer, Phys. Rev. D **46**, 2891 (1992), and references therein.
- [11] N. Isgur and C. Llewellyn Smith, Nucl. Phys. **B317**, 526 (1989).
- [12] T.-S. H. Lee, Argonne National Laboratory report PHY-5253-TH-88; T.-S. H. Lee, *Proceeding sof the International Conference on Medium and High Energy Nuclear Physics*, Taipei, Taiwan, 1988 (World Scientific, Singapore, 1988), p563; Y. Kang, P. Erbs, W. Pfeil, and H. Rollnik, *Abstracts of the Particle and Nuclear Intersections Conference*. (MIT, Cambridge, MA 1990); W. Pfeil, private communication; S. I. Nagornyi, Yu. A. Kasatkin, and I. B. Kirichenko. Yad. Fiz. **55**, 345 (1992) [Sov. J. Nucl. Phys. **55**, 189 (1992)].
- [13] M. Corcoran *et al.* Phys. Rev. D **22**, 2624 (1980).

[14] Hall A Line of Sight Shielding, CEBAF Tech Note TN-91-024, K. A. Aniol and V. Punjabi (1991); Low Energy Neutron Shielding for Hall A Detector Hut, K. A. Aniol, (1991), unpublished.

[15] A. Saha, private communication.

[16] C. Perdrisat, private communication. See also B. Bonin *et al.*, Nucl. Inst. Meth. **A288**, 379 (1990).

[17] T. Kamae *et al.*, Phys. Rev. Lett. **38**, 468 (1977); T. Kamae *et al.*, Nucl. Phys. **B139**, 394 (1978); H. Ikeda *et al.*, Phys. Rev. Lett. **42**, 1321 (1979); A. S. Bratashevskij *et al.*, Nucl. Phys. **B166**, 525 (1980); H. Ikeda *et al.*, Nucl. Phys. **B172**, 509 (1980); A. S. Bratashevskij *et al.*, Yad. Fiz. **32**, 418 (1980), [Sov. J. Nucl. Phys. **32**, 216 (1980)]; V. P. Barannik *et al.*, Nucl. Phys. **A451**, 751 (1986).

XI. FIGURE CAPTIONS

Figure 1: Cross sections for $d(\gamma, p)n$ at $\theta_{c.m.} = 90^\circ$ multiplied by s^{11} to exhibit the scaling behavior. The curve is the reduced nuclear amplitudes prediction of Brodsky and Hiller[4], normalized to the data at 1 GeV.

Figure 2: Cross sections for $d(\gamma, p)n$ at $\theta_{c.m.} = 37^\circ, 53^\circ,$ and 90° , multiplied by s^{11} to exhibit the violation of scaling at 37° . The curve is the same as for Figure 1.

Figure 3: Diagrams of pp scattering mechanisms. The asymptotic amplitude involves a single hard gluon exchange between the two nucleons. The Landshoff amplitude involves 3 independent hard gluon exchanges between the different quarks of the two nucleons. The asymptotic amplitude is short range – the quarks within each nucleon must be close together – and conserves quark and hadron helicities. Spatial separations between the quarks within each nucleon in the Landshoff amplitude allows nonzero orbital angular momenta, so that nucleon helicities may not be conserved, although quark helicities are.

Figure 4: Outgoing proton polarization measurements[17] in the $d(\gamma, p)n$ reaction at some angles. Some data points have been removed from regions with large numbers of data points, for clarity. The current experiment will triple the energy range of the data. The calculations at 90° are from Laget, and show sensitivity to the choice of deuteron wave function. Although the angles shown do not quite match the angles proposed in this experiment, we have added pseudodata to each plot, connected by lines, to show the results and uncertainties in the limits that asymptotic scaling applies at each point ($P = 0$), and that the polarization falls smoothly towards 0 by a factor of two over the energy range of the experiment (see text).

Figure 5: Total cross sections for γp and γd interactions, taken from Particle Properties Data Book.

Figure 6: pp polarization data, from Corcoran *et al.*[13].

Figure 7: Spin precession in HRS and SOS spectrometers. The dotted lines indicate the range of the proposed measurements.

Table 1 Kinematic points requested.

E_γ GeV	θ_{lab} deg	σ_{lab} nb/sr	rate ct/sec	$\theta_{precess}$ deg	time ¹ hours	statistical uncertainty
$\theta_{cm} = 37^\circ$						
0.75	25.2	184.0	1435.9	129.8	2	0.05
1.15	23.0	35.9	184.5	159.1	2	0.05
1.55	21.4	8.6	33.0	188.9	5	0.05
1.95	20.0	2.5	7.6	219.1	33	0.05
2.35	19.0	0.8	2.1	249.4	60	0.10
subtotal					102	
$\theta_{cm} = 53^\circ$						
0.75	36.6	166.6	1299.5	125.6	2	0.05
1.15	33.5	32.0	164.3	151.9	2	0.05
1.55	31.2	7.6	29.0	178.6	5	0.05
1.95	29.3	2.2	6.6	205.5	30	0.05
2.35	27.8	0.7	1.8	232.6	116	0.07
subtotal					155	
$\theta_{cm} = 90^\circ$						
0.75	65.9	114.6	894.3	112.7	2	0.05
1.15	61.0	20.7	106.4	129.8	3	0.05
1.55	57.3	4.7	17.9	147.0	11	0.05
1.95	54.2	1.3	3.9	164.2	32	0.05
2.35	51.6	0.4	1.0	181.3	151	0.05
2.75	49.4	0.1	0.3	198.5	135	0.10
subtotal					334	
$\theta_{cm} = 114^\circ$						
0.75	88.5	80.6	628.6	103.9	2	0.05
1.15	82.9	13.7	70.2	114.9	6	0.05
1.55	78.4	2.9	11.3	125.7	26	0.05
subtotal					34	
total					625	

¹ The time given includes time for the data, background subtractions, and overhead for angle and radiator changes.

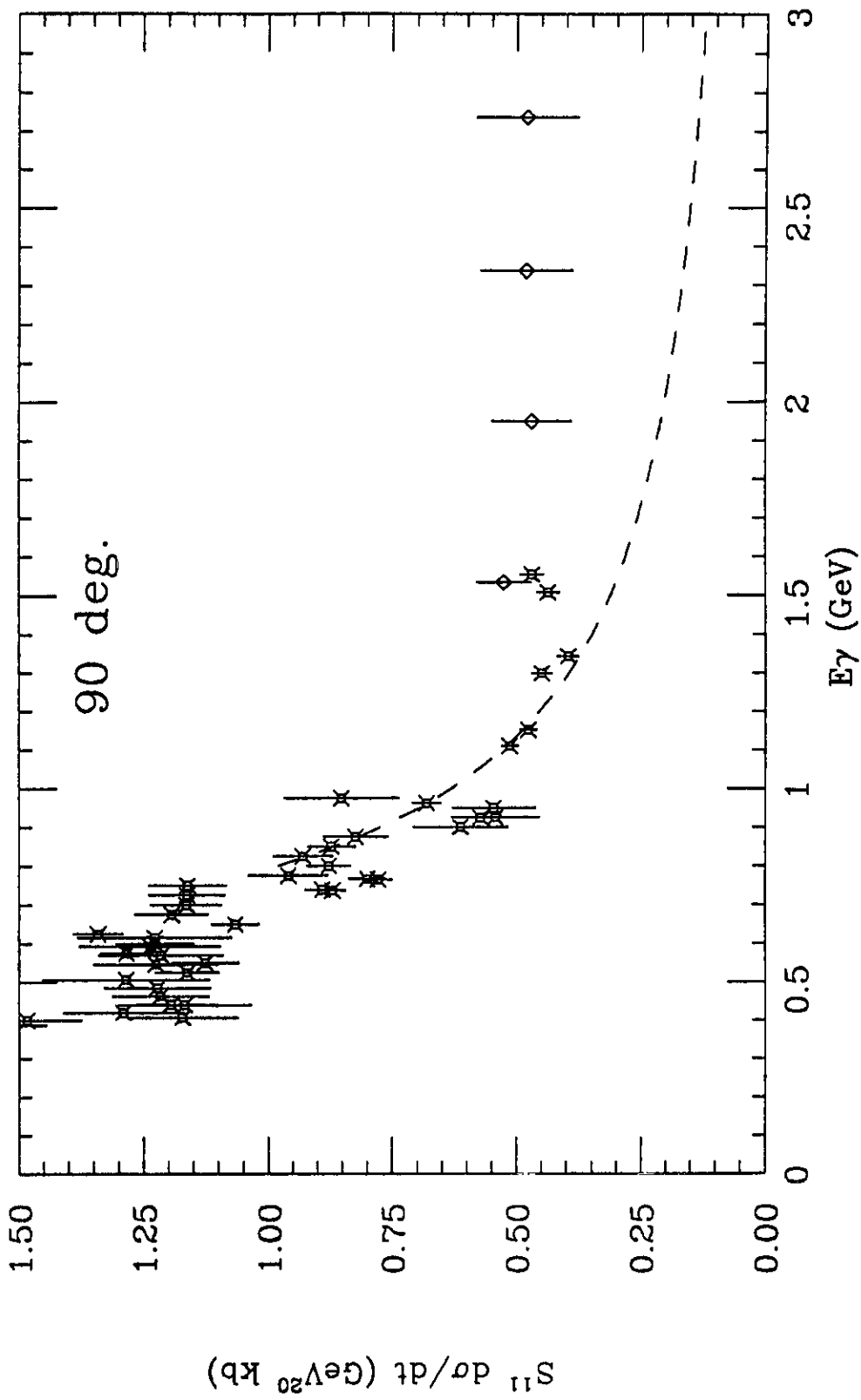


FIG 1

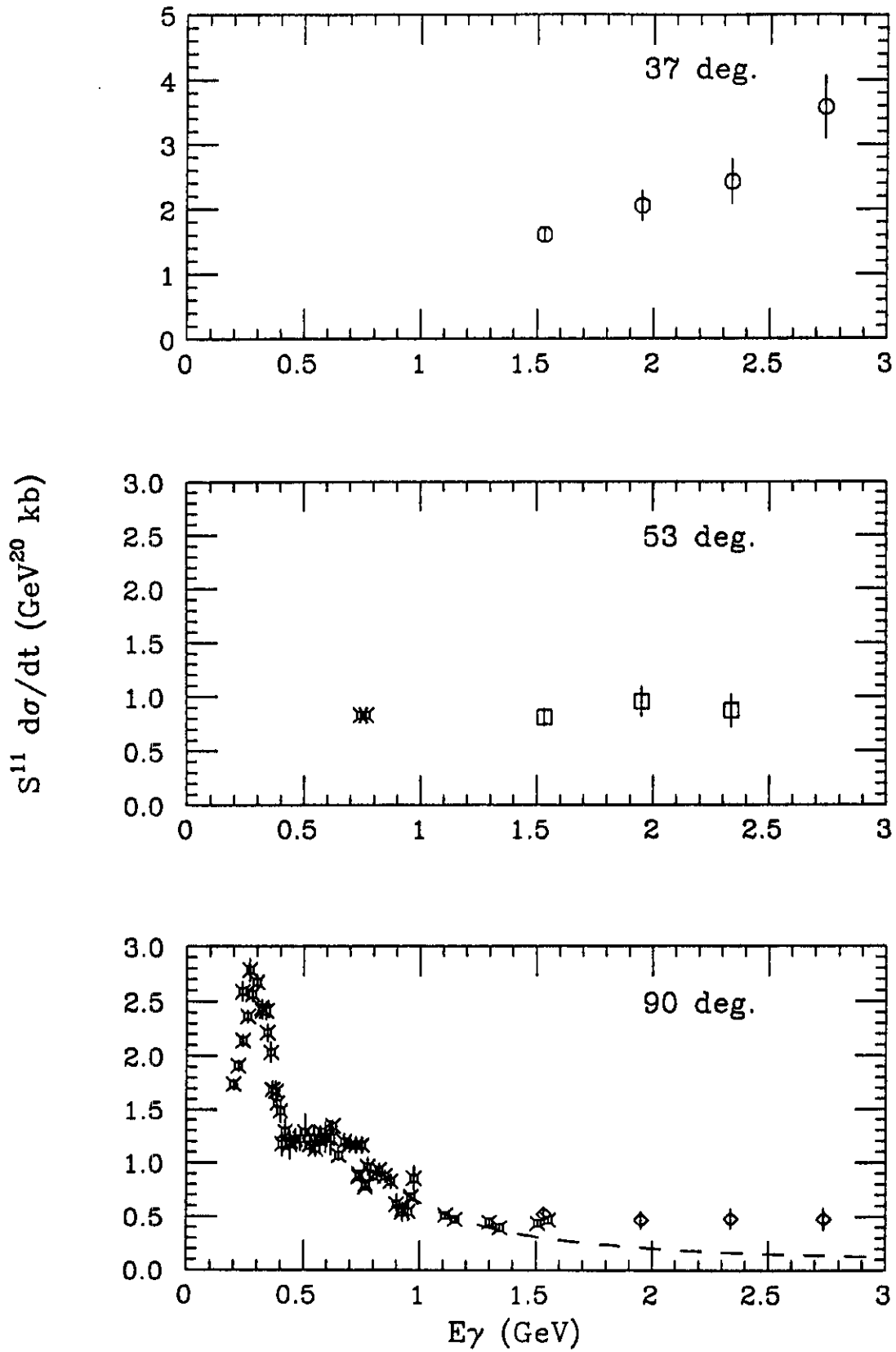
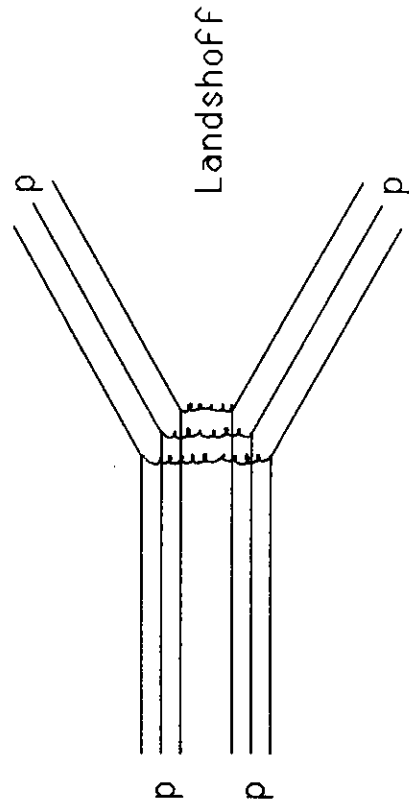
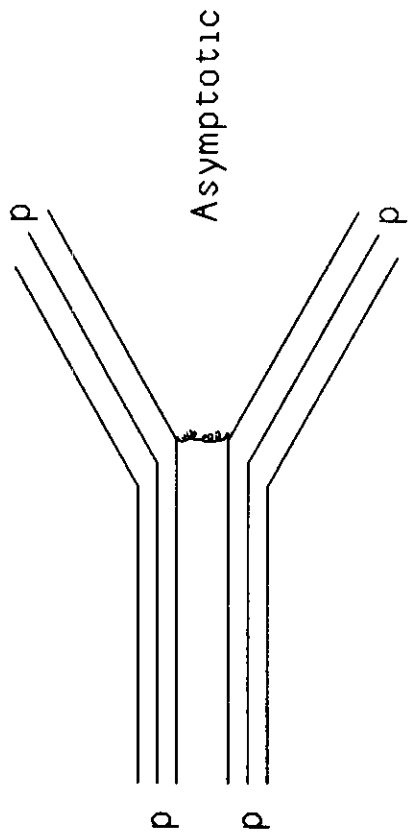


FIG 2



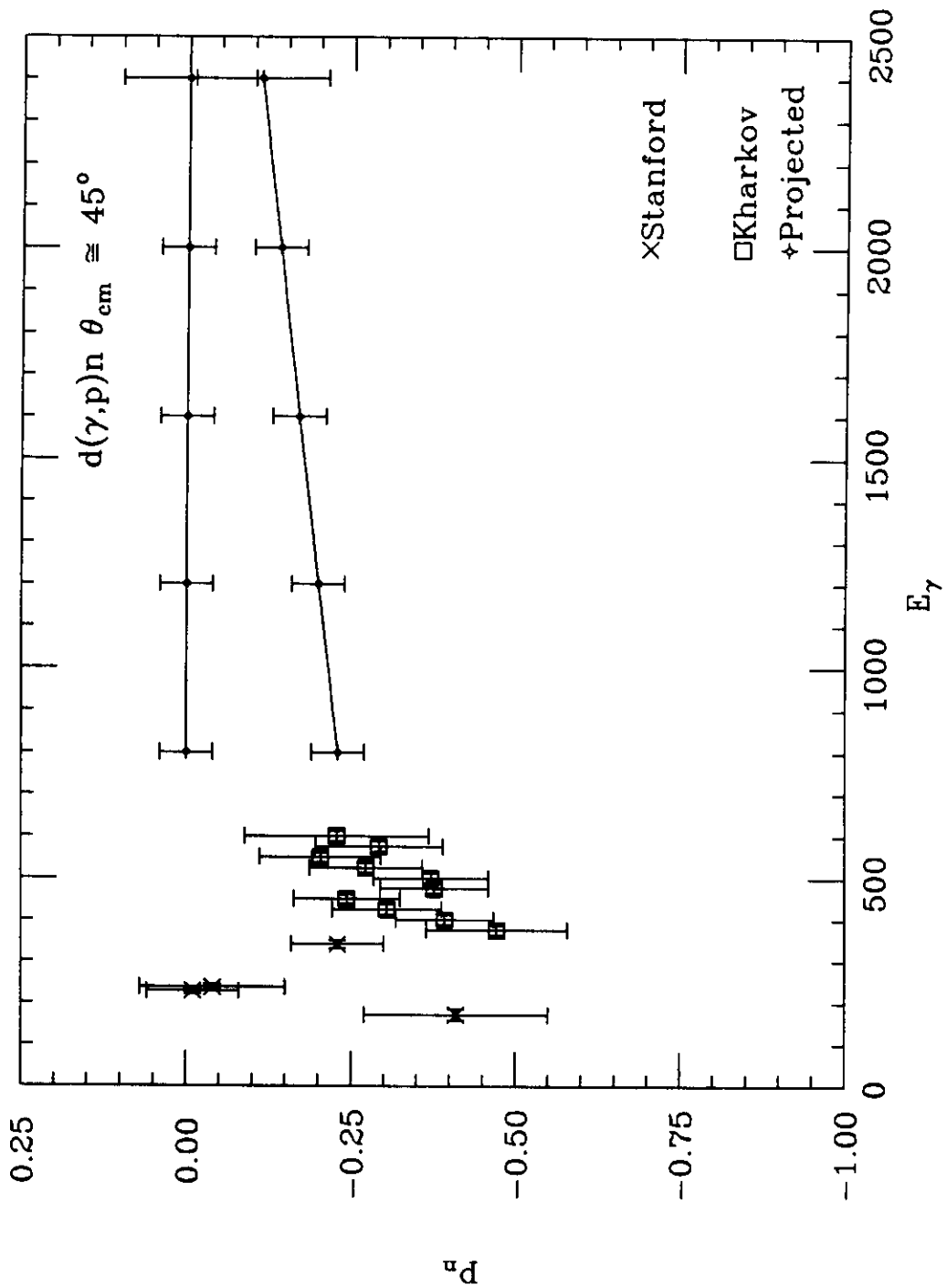


FIG. 4a

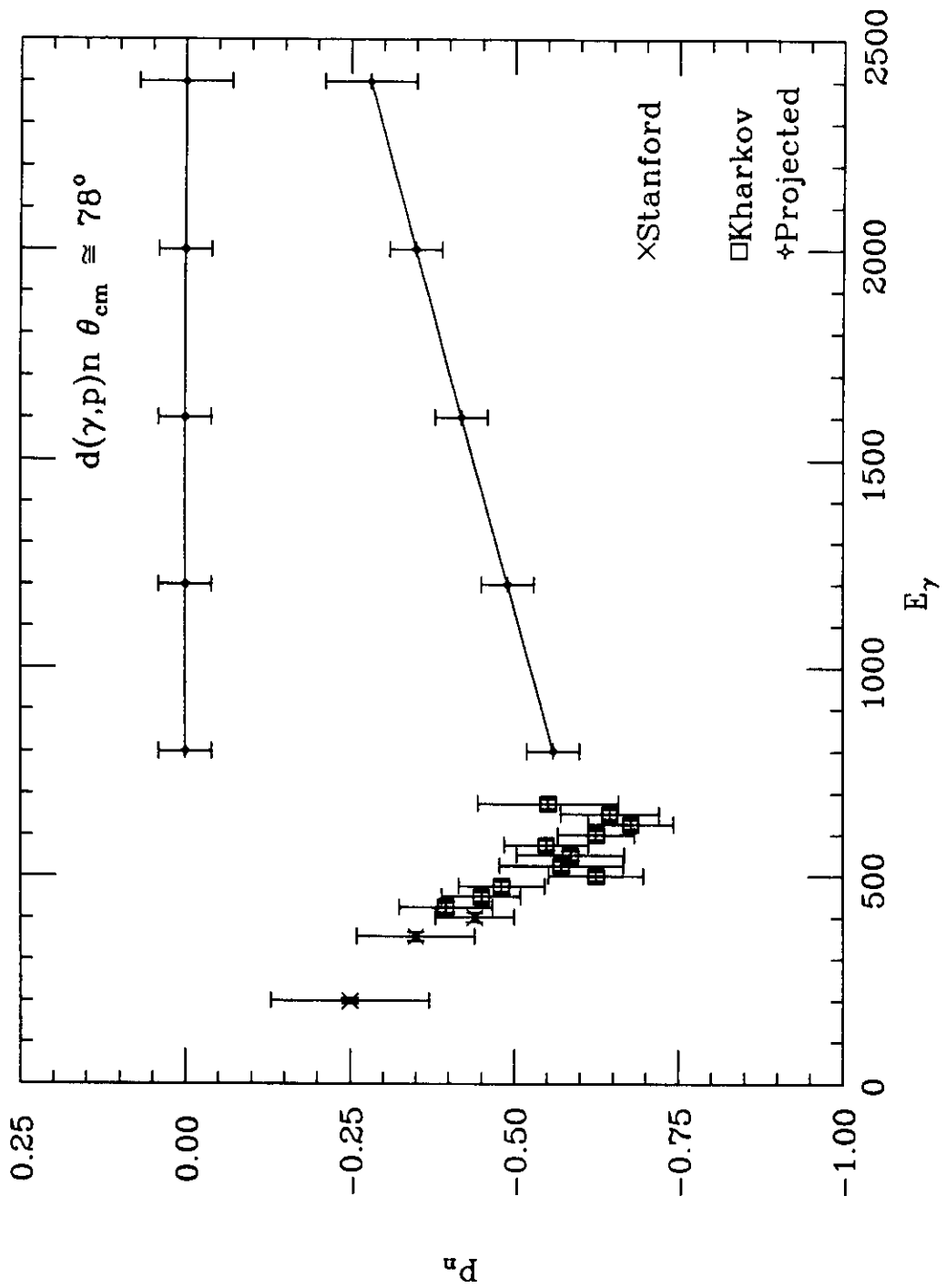
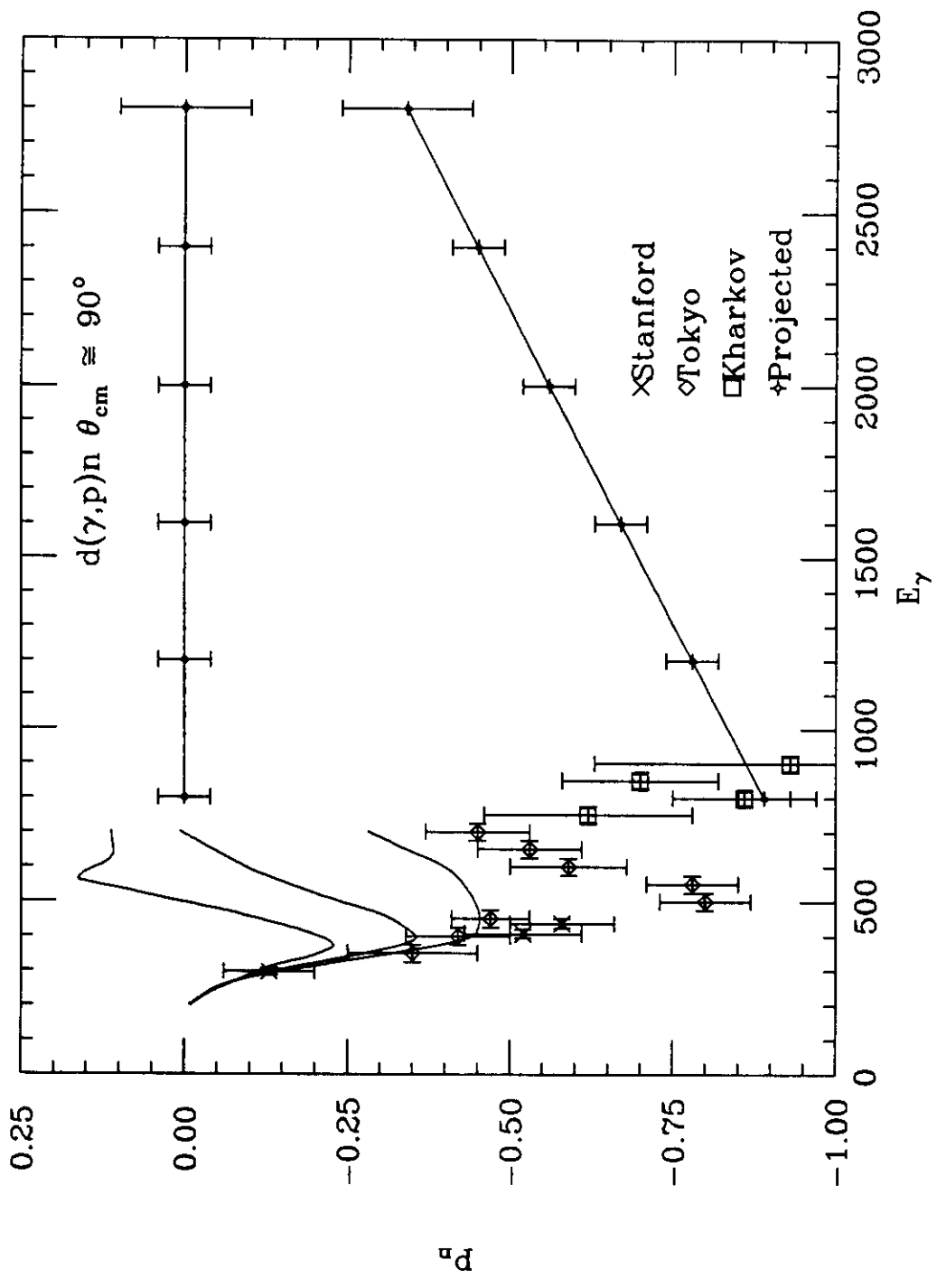


FIG. 4b



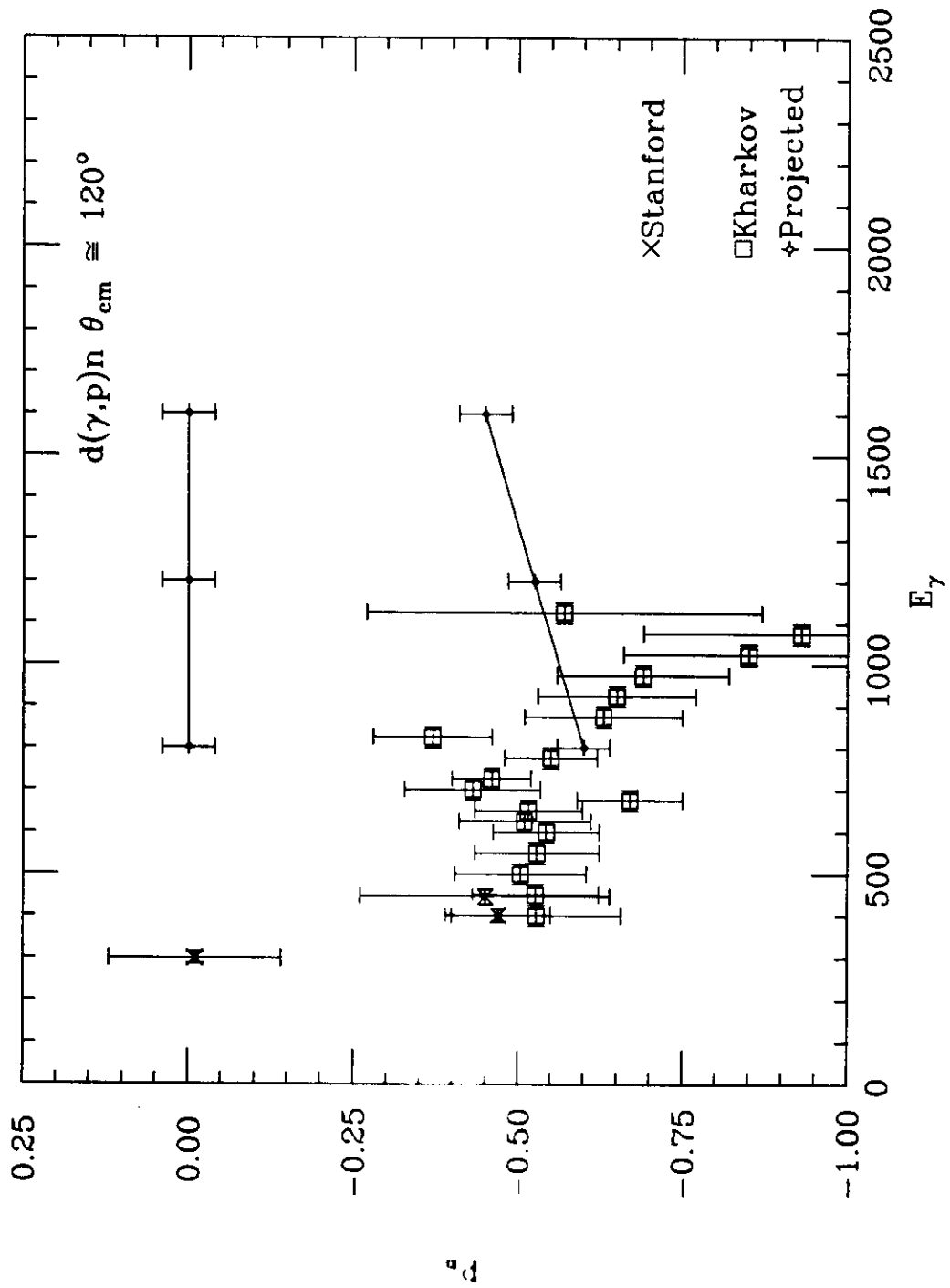
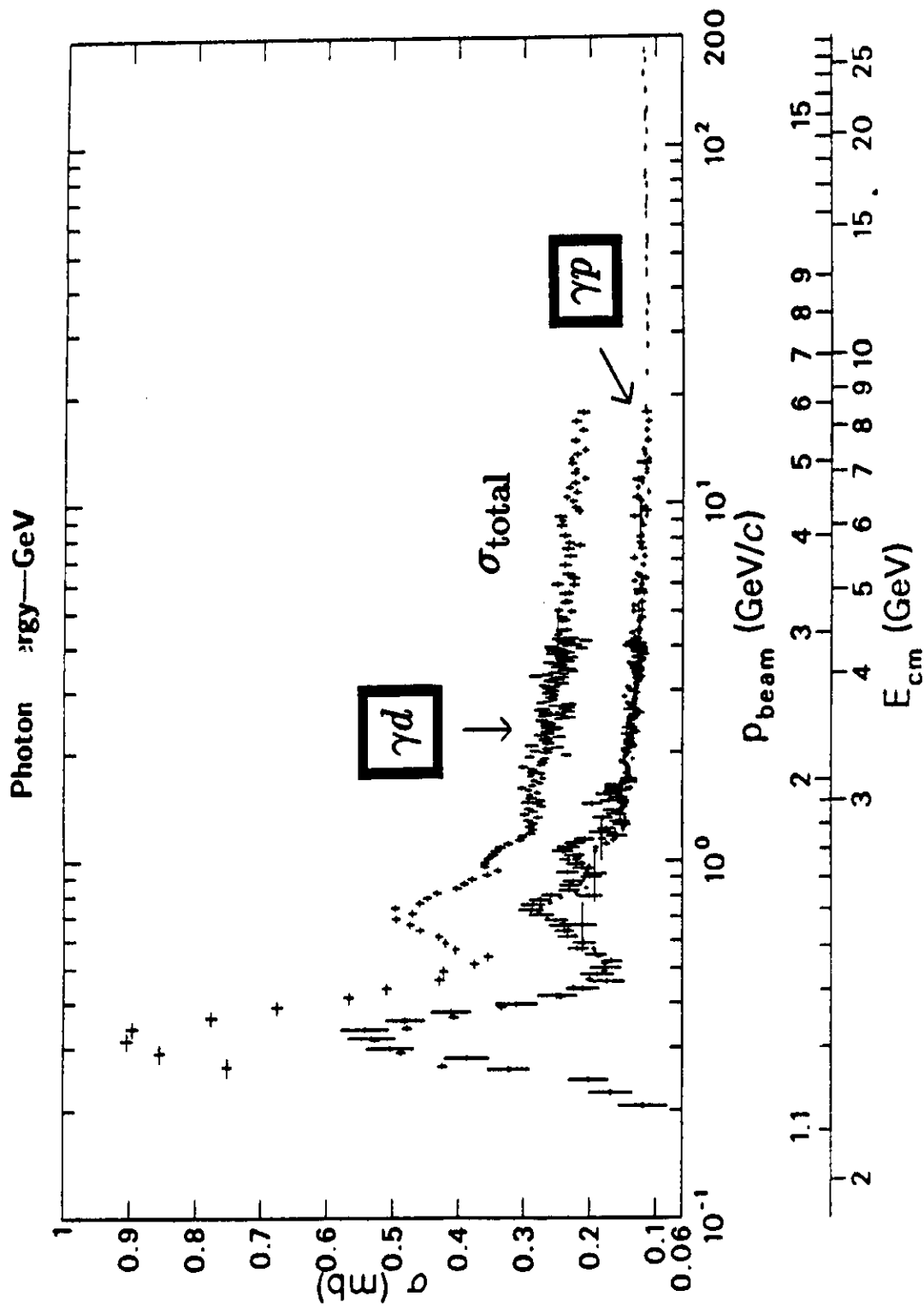


FIG 43



Photon cross sections vs. laboratory beam momentum p_{beam} and total center-of-mass energy E_{cm} . Data courtesy A. Baldini, V. Flaminio, W.G. Moorhead, and D.R.O. Morrison, CERN; COMPAS Group, IHEP, Serpukhov, USSR; and G.M. Lewis, Glasgow. See *Total Cross-Section for Reactions of High Energy Particles*, Landolt-Bornstein, New Series, Vol. 12a and 12b, H. Schopper, Ed. (1987).

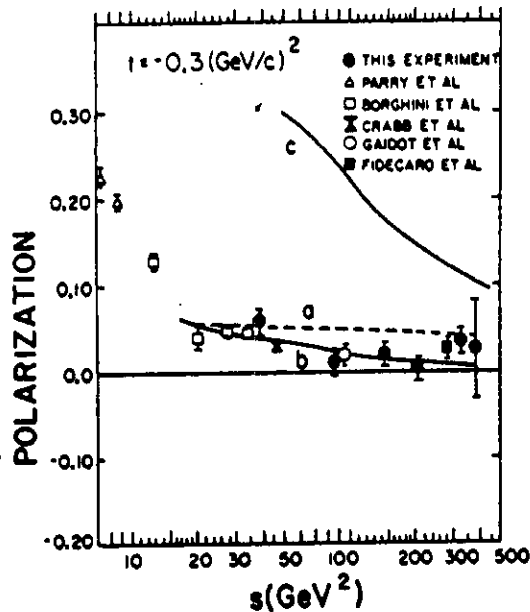


FIG. 12. Elastic proton polarization as a function of s for $-t = 0.3 (\text{GeV}/c)^2$. Curve a , Pumplin and Kane (Ref. 16); curve b , Gerhold and Majerotto (Ref. 14); curve c , Wu, Bourrely, and Soffer (Ref. 17).

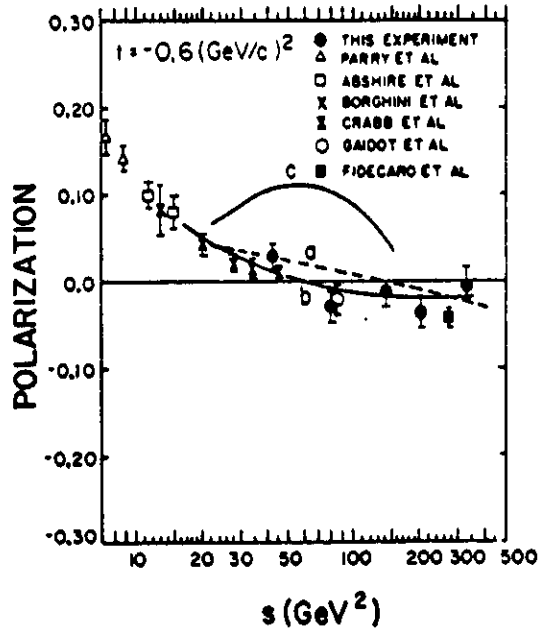


FIG. 13. Elastic proton polarization as a function of s for $-t = 0.6 (\text{GeV}/c)^2$. Curve a , Pumplin and Kane (Ref. 16); curve b , Gerhold and Majerotto (Ref. 14); curve c , Wu, Bourrely, and Soffer (Ref. 17).

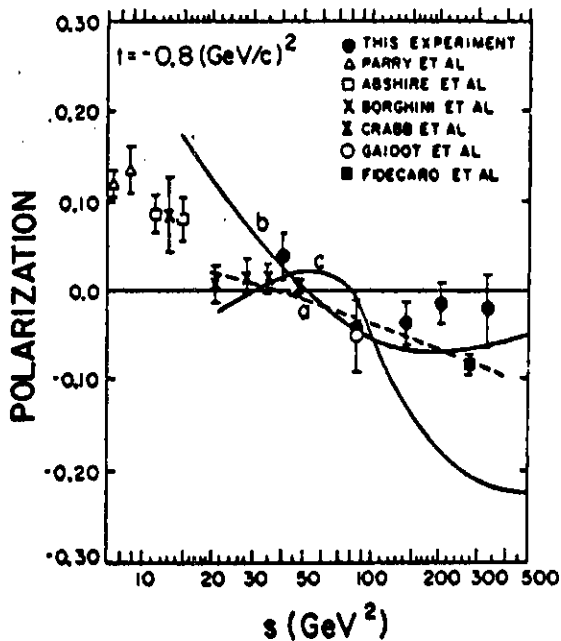


FIG. 14. Elastic proton polarization as a function of s for $-t = 0.8 (\text{GeV}/c)^2$. Curve a , Pumplin and Kane (Ref. 16); curve b , Gerhold and Majerotto (Ref. 14); curve c , Wu, Bourrely, and Soffer (Ref. 17).

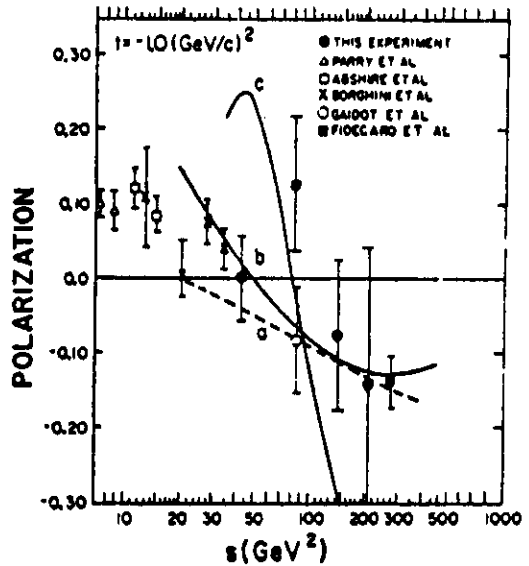


FIG. 15. Elastic proton polarization as a function of s for $-t = 1.0 (\text{GeV}/c)^2$. Curve a , Pumplin and Kane (Ref. 16); curve b , Gerhold and Majerotto (Ref. 14); curve c , Wu, Bourrely, and Soffer (Ref. 17).

Spin precession in spectrometers

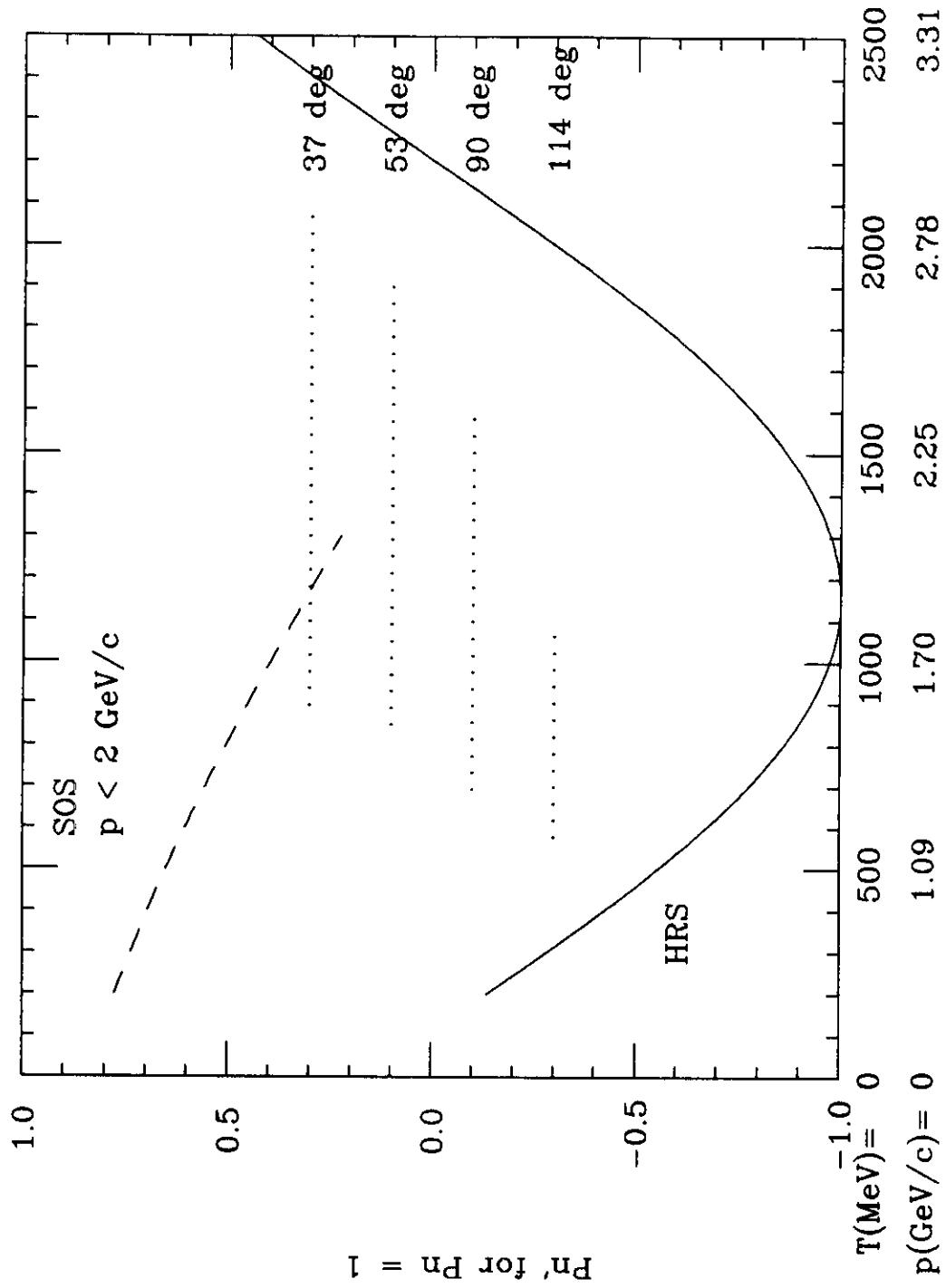


FIG 7